RESERVOIR CHARACTERISATION OF THE MIDDLE MIOCENE CA VOI XANH ISOLATED CARBONATE PLATFORM

Christian J.Strohmenger[1,3], Lori Meyer[2], David S.Walley[1], Mazlina Md Yusoff[1], Donald Y.Lyons[1], Jacqueline Sutton[1], John M.Rivers[4] Beata von Schnurbein[3], Nguyen Xuan Phong[5]
[1]Esso Australia Pty. Ltd.
[2]ExxonMobil Exploration & Production Vietnam Ltd.
[3]ExxonMobil Production Germany GmbH
[4]ExxonMobil Research Qatar
[5]Petrovietnam Exploration Production Corporation
Email: christian.j.strohmenger@exxonmobil.com

Summary

The Ca Voi Xanh field is located offshore Vietnam in the southern Song Hong basin. Tertiary carbonates of Middle Miocene (Langhian and Serravallian) age form an isolated carbonate platform on top of the Triton Horst structural high. Shallow water corals and large and small benthic foraminifera are the main constituents of the older Langhian carbonates, whereas the overlying Serravallian carbonates are dominated by deeper water coralline red algae (rhodolith) and large benthic foraminifera (LBF).

Sequence stratigraphic interpretation is based on detailed sedimentolological core description tied to well-log character. A sequence stratigraphic framework was established for the Serravallian carbonates, displaying three third-order depositional sequences (Ser1, Ser2, and Ser3).

Langhian carbonates can be described by one lithofacies: coral-LBF-foraminifera grainstone-packstone/rudstone. Depending on the presence of mud in the samples, two lithofacies types are characteristic for the Serravallian: LBF-rhodolith packstone to mud-lean packstone and rhodolith-LBF grainstone to mud-lean packstone.

Two well-developed exposure surfaces can be identified on top of the Langhian (Serravallian sequence boundary Ser1_SB) and on top of the Serravallian (Tortonian sequence boundary Tor1_SB). Serravallian carbonates show an overall shallowing-upward trend from more horizontally-oriented coralline red algae (encrusted and bored pavements/hardgrounds) at the lower part of the section to large, roundish, irregular rhodoliths towards the upper part of the section. Petrographic thin section, stable isotope (oxygen and carbon), and fluid inclusion analyses confirm a freshwater (vadose and phreatic) diagenetic overprint of the carbonates below the exposure surfaces (sequence boundaries).

Partial dolomitisation observed at Well-2 and Well-3 might be related to CO_2 and hydrocarbon charging, causing secondary leaching of the Mg-rich coralline red algae and LBFs; leading to an enrichment of the water with Mg-ions and thus favouring downward dolomitisation of the Serravallian carbonates.

A reproducible reservoir rock type (RRT) scheme was developed for the described carbonates, using a combination of depositional environment, diagenetic overprint, and reservoir parameters (porosity and permeability). The Langhian is characterised by two RRTs, depending on the degree of cementation (RRT-3L) and dissolution (RRT-5L). The Serravallian RRTs are separated into dominantly packstone (RRT1) and dominantly grainstone textures (RRT-2, RRT-3, RRT-5, and RRT-6). RRTs with grainstone texture show varying degrees of cementation (RRT-2 and RRT-3) and dissolution (RRT-5 and RRT-6). Early diagenetic dolomitisation (RRT-4) preferentially effects packstone (RRT-1), but also grainstone textures (RRT-3 and RRT-5). The vertical and lateral distribution of RRTs, supported by seismically-derived paleo-reconstruction of the carbonate platform, adequately describes the reservoir.

The geologic (static) model consists of both, matrix and non-matrix components. Seismically-derived probablitiy maps for each of the six Seravallian RRTs, based on 3D seismic paleo-structure mapping, were used as input to the matrix component of the geologic model. Different karst geometries and features consistent with known hydro-geologic processes are identified in the seismic discontinuity (variance) cube and are used to interpret karst regions with different degrees and/or types of karst/fractures. These karst regions are used to populate the non-matrix component of the geologic model along the identified two major sequence boundaries (Ser1_SB and Tor1_SB).

Key words: *Reservoir characterisation, carbonate platform, Ca Voi Xanh field.*

Date of receipt: 16/5/2018. Date of review and editing: 16 - 17/5/2018. Date of approval: 18/5/2018.

1. Introduction

The Ca Voi Xanh field is located offshore Vietnam in the southern part of the Song Hong basin, between the Qiongdongnan basin in the north and the Phu Khanh basin in the south [1, 2]. The greater East Sea area has a relatively simple tectonic history. In the Eocene to Early Oligocene, extension (rifting) was initiated, followed by movements along the Red River/East Vietnam Boundary Fault Zone approximately 45 million years ago. The Red River Fault is a major left-lateral strike-slip fault system caused by the collision of the India and Asia tectonic plates. Motion on the Red River Fault System continued into the Early Miocene, and marine conditions, triggering carbonate platform growth, were established East of the fault zone on top of structural highs. Carbonate growth was widespread on structural highs offshore Central Vietnam throughout the Early and Middle Miocene. Regional uplift of the mainland resulted in increased influx of siliciclastics from the West; leading to stressed carbonate growth and finally to the drowning of the Tri Ton horst carbonate platform during the Late Miocene [1, 2].

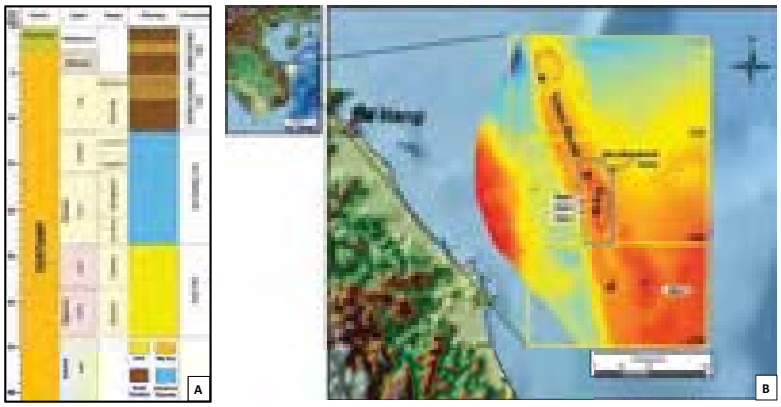

Figure 1. *Generalised stratigraphic column for the Tri Ton horst area (a). Regional top carbonate depth map showing Tri Ton horst high (bright red colors), Blocks 117 through 119 (yellow outlines), and the location of the four exploration wells. Also shown are the offshore Ca Voi Xanh field area (red outline) and the remaining development area (blue outline) (b).*

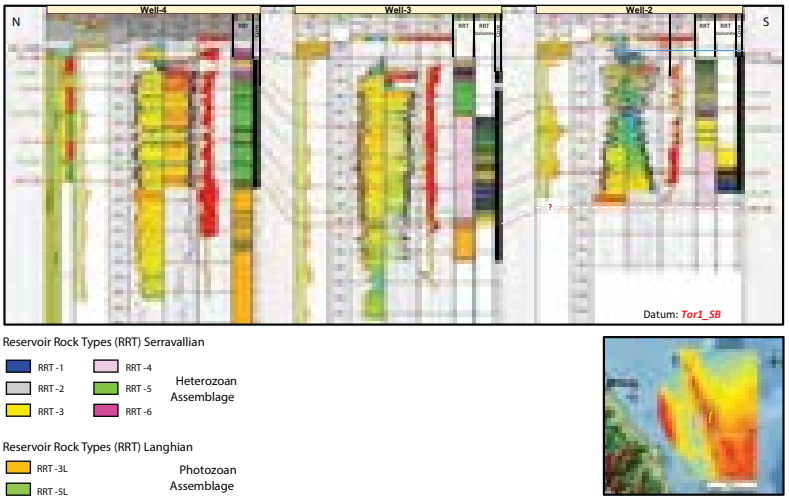

Figure 2. *Serravallian sequence stratigraphic framework showing sequence boundaries (SB) in red, flooding surface/sequence boundary (FSSB) in blue, and maximum flooding surfaces (MFS) in green. The logs displayed for each well are Gamma Ray (Track 1), Porosity (Track 2), Permeability (Track 3), and Neutron-Density (Track 4). Vertical reservoir rock type (RRT), and pre-dolomite rervoir rock type (RRT Dolomite) distribution, as well as the cored interval (Core) is displayed for each well.*

The generalised stratigraphy of the region is shown on Figure 1a. Middle Miocene age carbonate platforms of the Da Nang Formation nucleated on older, remnant syn-rift highs. The Ca Voi Xanh platform is an isolated carbonate platform that was established on the Tri Ton horst structural high (Figure 1b). The horst is a positive feature separated in the West from land by a deep trough that trapped time-equivalent clastics and allowed deposition of carbonates on the Tri Ton horst structural high. Carbonate deposition ended when clastics filled the trough and prograded over the carbonate platform.

2. Sequence stratigraphy

The complete carbonate interval at Ca Voi Xanh and south of Ca Voi Xanh was penetrated by two wells, where it is approximately 600 to 800m thick. The well penetrations in the main Ca Voi Xanh platform (Well-2, Well-3, and Well-4) only penetrated the upper portion (less than 200m) of the carbonate platform. Well-3 and Well-4 were cored across the Serravalian sequence boundary Ser1_SB into the Langhian section. The core obtained from the Well-2 only covers the Serravallian interval (Figure 2).

Sequence stratigraphic correlation between Well-2, Well-3, and Well-4 is based on observed facies distribution, biostratigraphic interpretation, and well-log character. Conventional core was recovered from all three wells, in addition to sidewall cores from Well-2 and Well-4. A sequence stratigraphic framework was established for the Serravallian carbonates. The Serravallian interval can be described by one third-order composite sequence [3], comprising three

third-order depositional sequences: Ser1, Ser2, and Ser3 (Figure 2). Four major regionally correlative surfaces can be carried across the Ca Voi Xanh platform: Serravallian sequence boundary Ser1_SB (identified on well-logs, core, and seismic), Serravallian maximum flooding surface Ser2_MFS (identified on well-logs and core only), Tortonian sequence boundary Tor1_SB (identified on well-logs, core, and seismic), and Tortonian flooding surface/sequence boundary Tor1_FSSB (identified on well-logs and core only), merging with the Tor1_SB at Well-2 and Well-3. The Ser2_MFS (Serravallian third-order composite maximum flooding surface) correlates with a zone of bioturbated hardgrounds with platy corals observed in core material of all three wells and is closely associated with an elevated gamma ray response (Figure 2). Generally, above the third-order composite Ser2_MFS, Serravallian carbonates show decreasing (lower) GR-log values, compared to Serravallian carbonates below the Ser2_MFS (Figure 2).

Langhian carbonates, directly underlying the Serravallian third-order sequence boundary Ser1_SB display root marks filled with detrital quartz grains, indicative of an exposure surface [4] (Figure 3). Serravallian carbonates show a cemented interval of varying thickness, interpreted to be the result of exposure, directly below the third-order Tortonian sequence boundary Tor1_SB (Figure 4a). Glossifungites burrows, as well as fluid inclusion (brackish to fresh water inclusions) and stable isotopes (typical "inverted J" trend of oxygen and carbon isotopes [5, 6]; Figure 4b) analyses support the interpretation of an exposure surface, related to a sea-level lowstand at the end of Serravallian time.

The Tor1_SB at Well-4 (top of cemented zone, approximately 10m below the top carbonate) is correlated with the top carbonate picks at Well-2 and Well-3 (Figure 2). The interpreted Tor1_FSSB, marking the top carbonate at Well-4, merges with the Tor1_SB in the other wells (absence of uppermost, approximately 10m thick carbonate succession; Figure 2).

Figure 2 shows the above described integrated stratigraphic framework on a North-South oriented well cross-section.

3. Environment of deposition

The Environment of Deposition (EOD) interpretation is based on the integrated sequence stratigraphic framework, the antecedent topography, and biostratigraphic analyses, mostly done on large benthic foraminifera (LBF) and coralline red algae (rhodoliths).

Langhian-age deposits are interpreted to inherit a broad central platform morphology based on core-interpreted facies and seismic facies analysis across the platform. Serravallian deposits are interpreted to occupy a wide facies belt associated with a central platform high. The depositional style changes between Langhian (rimmed platform) and Serravallian (carbonate ramp) time. Both, Langhian and Serravallian carbonates were exposed during sea-level lowstands at the end of Langhian and Serravallian times.

During the Langhian, the common presence of hermatypic coral rudstones, interlayered with packstones, and grainstones, rich in large benthic (Miogypsina) and, predomminantly, small benthic foraminifera, including miliolids, soritids, and alveolinids point to a warm, shallow marine, inner shelf environment of deposition [7]. Coral-rich patch reefs can be found forming today in many platform-interior, shallow, warm, well-lit settings [8, 9]. Langhian carbonates represent a typical photozoan association of organisms [9].

The Serravallian third-order composite sequence is interpreted to represent a deeper open marine, proximal to distal middle ramp environment [11]. The carbonates are rich in large benthic foraminifera (LBF) like Cycloclypeus, Katacycloclypeus, Amphistegina, and Lepidocyclina, coralline red algae with encrusting foraminifera (Acervulina inhaerens), and minor small benthic and planktonic foraminifera. In contrast to the Langhian, Serravallian carbonates represent a typical heterozoan association of organisms [10].

Coralline red algae (Corallinales, Halidiales and Sporolithales, Rhodophyta) are common and are represented by members of the subfamilies Neogoniolithoideae, Mastophoroideae, Melobesioideae, and Lithophylloideae (family Corallinaceae), and members of the families Hapalidiaceae and Sporolithaceae. Six non-geniculate genera (seven species) of coralline red algae were recognised. Neogoniolithoideae: Neogoniolithon and Spongites; Mastophoroideae: Lithoporella; Lithophylloideae: Lithophyllum; Melobesioideae: Mesophyllum and undetermined melobesioids; Sporolithaceae: Sporolithon [11].

Coralline red algae occur as encrusting thalli floating in the sediment matrix, rhodoliths, as well as thallial fragments. Rhodolith shapes range from sub-spheroidal

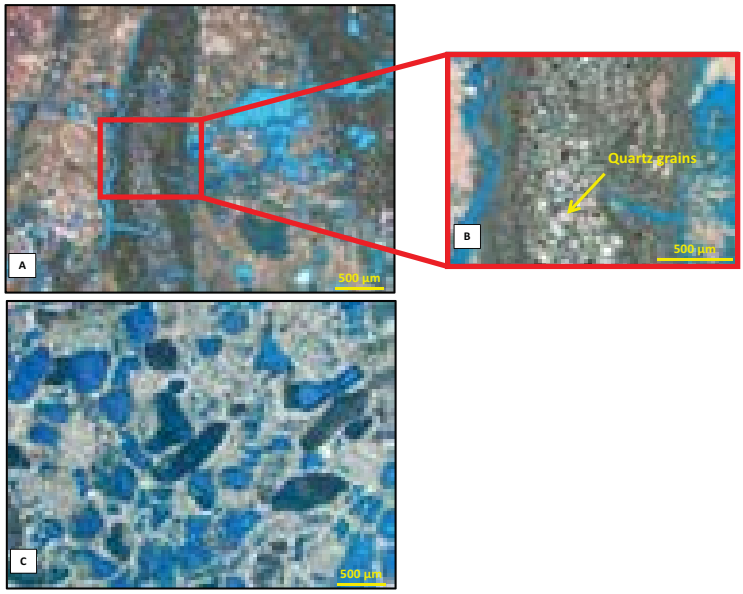

Figure 3. *Thin section photomicrograph (below Serravallian sequence boundary Ser1_SB) showing probable root traces filled with quartz grains (pedogenic overprint) (a). Close-up of Figure 3a (b). Thin section photomicrograph (below Serravallian sequence boundary Ser1_SB) showing dissolution of less-stable bioclasts and cementation of original interparticle pore space (porosity inversion) (c).*

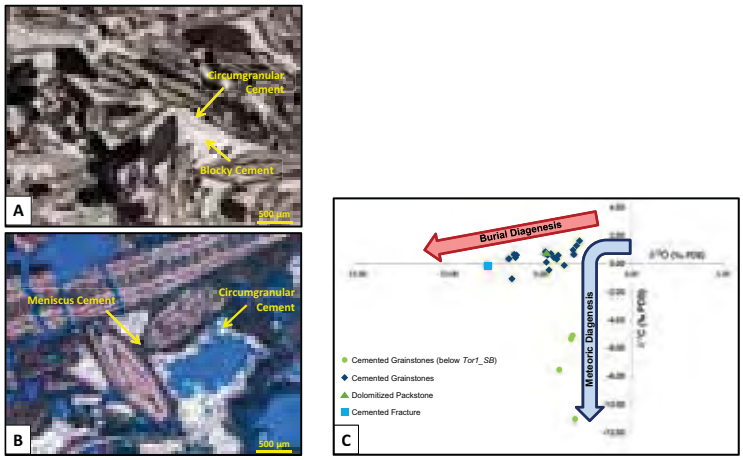

Figure 4. *Thin section photomicrograph (below Tortonian sequence boundary Tor1_SB) showing meteoric phreatic circumgranular and blocky cement (a). Thin section photomicrograph (below Tortonian sequence boundary Tor1_SB) showing vadose cryptocrystalline meniscus cement, overgrown by meteoric phreatic circumgranular cement (b). Stable isotope analyses ($\delta^{18}O$ and $\delta^{13}C$) confirm the interpreted meteoric origin of cement types displayed on Figure 4a (green dots; blue, "inverted J" trend). Most samples show the burial (red) trend (c).*

to flat shapes. Inner and outer parts of the rhodolith do not show different growth-forms. Encrusting growth-forms are very common in the outer parts of the rhodoliths. Rare warty morphologies are also present. Encrusting foraminifera are represented by acervulinids which, together with the coralline red algae, make up rhodoliths and the encrusting coralline framework (i.e., crustose pavement). Acervulinids can be dominating and often alternate with coralline red algae making superimposed successions of coralline thalli/acervulinid shells [11].

Coralline algae can be common in both tropical and non-tropical settings, though they seem to be more prevalent as facies dominating components in the latter. In the studied thin sections, reef-building corals and dasycladalean green algae are missing; suggesting that these deposits may represent a tropical/warm temperate water transitional area. Non-tropical heterozoan carbonates do not form carbonate platforms with steep, wave-resistant rims, but can accumulate hydrodynamically as carbonate ramps.

The coralline red algal and larger foraminiferal assemblages suggest deposition in environments between (below) fair-weather wave base (FWWB) and storm wave base (SWB), or what is referred to as the middle ramp setting [12 - 15]. This setting was further differentiated based on gradient ranging from: (1) the proximal middle ramp or shallowest part close to the FWWB and characterised by higher coralline taxonomic diversity and abundant larger nummulitid foraminifera to (2) the distal middle ramp, representing the transition to the outer ramp, characterised by lower coralline taxonomic diversity, dominated by melobesioids, and larger orbitoidiform foraminifera [11].

The dominance of Neogoniolithoideae in shallow water settings with an increase in the presence of Melobesioideae with depth has been observed in many areas including the Hawaiian Islands [16], Ryukyu Islands [17 - 19], Papua New Guinea [20], Gulf of Mexico [21, 22], Rio de Janeiro [23], and South Pacific reefs [22]. The sporolithacean Sporolithon occurs from tropical to temperate areas [25 - 27] from sea-level down to 80m water depth [16, 25, 28 - 30].

Middle Miocene sediments with abundant rhodoliths (composed of Lithothamnion and Sporolithon) from the Queensland Plateau and Marion Plateau are believed to be deposited in water depths between 30 and 80m [14, 15, 31].

On the Kikai-jima shelf (Central Ryukyu Islands, Japan), at water depths of 61 to 105m, sandy and gravelly carbonate sediments are characterised by macroid pavements

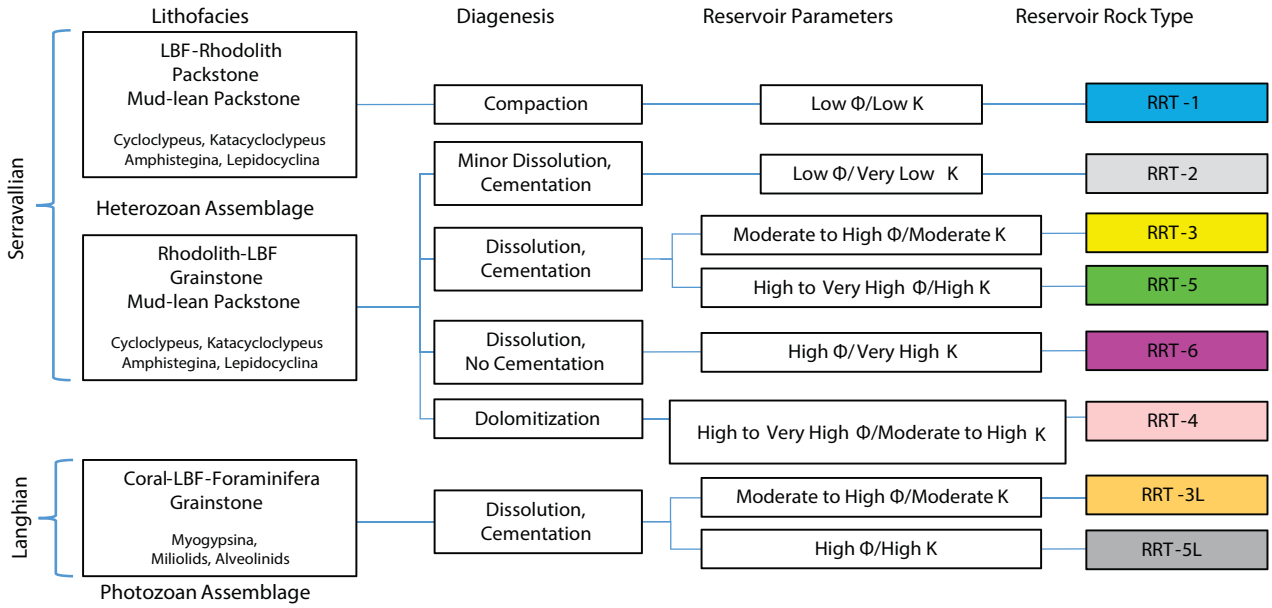

***Figure 5**. Langhian and Serravallian Reservoir Rock Types tied to lithofacies, diagenesis, and resulting reservoir parameter.*

[32]. Macroids, ranging in size from ca. 25 to 130mm in diameter, are spheroidal and sub-spheroidal in shape and consist mainly of the encrusting foraminifera Acervulina inhaerens and subordinate thin encrusting and lumpy coralline algae. The macroid pavements are forming under low sedimentation rates and occasional movement due to current action. Similar environmental characteristics can be argued for the studied material. The occurrence of the ichnotaxa Gastrochaenolites and Entobia confirm a low sedimentation rate of the setting.

Crustose pavements consist of coralline algal bindstone made up of thin encrusting coralline thalli, superimposed onto each other. The framework points to low turbulence interpreted to be in the distal portion of the middle ramp. Somewhat contradicting, the pavement is also characterised by Neogoniolithon.

Also Rhodolith beds are sites of biodiversity, they are habitats hampering the occurrence of larger foraminifera. The dominance of acervulinids and melobesioids can be indicative of a middle ramp, below 50m water depth (a similar setting in which the Kikai-jima macroids grow; low sedimentation rate, occasional overturning [32]). However, the occurrence of Neogoniolithon suggests a shallower setting. The occurrence of Neogoniolithon both in the crustose pavement and in rhodolith beds could correlate to two settings, located not very far from each other. Within the proximal to distal middle ramp, the crustose pavement occur in a low energy, deeper water area, whilst the rhodolith beds in an occasionally turbulent, somewhat shallower setting.

The depositional system of the analysed thin-section material is interpreted as a ramp. The environment of deposition ranges from a proximal middle ramp, relatively shallow-water setting below the FWWB, to a distal middle ramp, realtively deeper-water setting with occasional high water motion (storms) causing rhodolith overturning. An inner ramp setting is ruled out due to (1) the absence of very shallow-water coralline taxonomic assemblage and components such as hermatypic corals, abundant larger porcellaneous foraminifera and dasycladaleans green algae, and (2) the abundant occurrence of orbitoidiform larger foraminifera (typical of middle-outer ramp environment).

A summary of the rhodoliths identified and their general paleogeographic setting [11] are:

Proximal Middle Ramp

- Dominated by Mastophoroideae (Lithoporella) and Neogoniolithoideae (Neogoniolithon, Spongites)

- Subordinate corallines such as Melobesioideae (Mesophyllum), Lithophylloideae (Lithophyllum) and Sporolithaceae (Sporolithon)

- Higher coralline taxonomic diversity

- Occurrence of nummulitid larger foraminifera

- Occurrence of larger porcellaneous foraminifera (Orbitolites, Neoplanorbulinella)

Distal Middle Ramp

- Dominated by Melobesioideae (Mesophyllum)

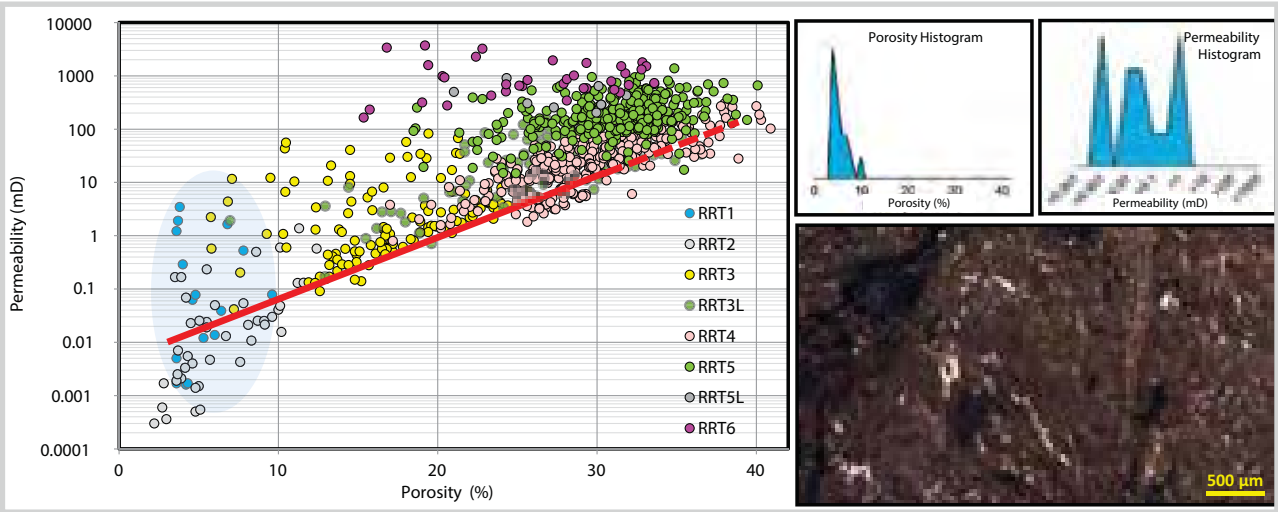

Figure 6. *Reservoir rock type 1. Displayed are permeability/porosity cross-plot (left) and porosity and permeability histograms, as well as thin section photomicrograph (right). Microporosity line (red), showing microporosity-dominated (below the red micro porosity line) and non-microporosity-dominated (above the red microporosity line) samples [40, 41].*

- Subordinate corallines such as Mastophoroideae (Lithoporella), Neogoniolithoideae (Neogoniolithon, Spongites), and undetermined melobesioids

- Lower coralline taxonomic diversity

- Bioerosion by boring sponges (Entobia) and bivalves (Gastrochaenolites)

A likely average paleo-water depth for the Serravallian sediments is interpreted to be between 50 and 80m (distal middle ramp) below Ser2_MFS, and < 80m, shallowing-upward to approximately 30m above Ser2_MFS; towards the top of the reservoir (Tor1_SB).

The Serravallian carbonate section is overlain by Tortonian, deeper marine, outer ramp, marls or claystones with > 90% planktonic foraminifera.

4. Diagenesis

Detailed analysis of core and thin section material has led to an understanding of the paragenetic sequence for the Serravallian carbonate reservoir that highlights the importance of diagenetic overprint rather than primary deposition on reservoir parameter trends.

Alteration of Ca Voi Xanh carbonate sediments began in the marine realm soon after deposition (both in Langhian and Serravallian times). Early seafloor alteration of sediments is apparent in most thin sections in the form of grain micritisation and micritic envelope formation. These alterations occur through the activity of bacteria and algae borings into grains. Thin isopachous fibrous, marine cements (neomorphosed aragonite cement) are present in some Ca Voi Xanh thin sections, but are volumetrically insignificant. More common are isopachous bladed, marine cements (neomorphosed high-Mg calcite cement). Neither grain micritisation nor seafloor cementation has a major impact on reservoir quality. Notably missing in the Serravallian sequence are large numbers of original aragonitic allochems (green algae, molluscs, and corals). Importantly, the Serravallian fossil assemblage is rich in Mg-calcite, as both the rhodoliths [10] and the large benthic foraminifers such as Amphistegina [33] are composed of this mineral.

Meteoric diagenesis (both vadose and phreatic) follows early sediment alteration (Figure 4). There are two important aspects to this alteration with respect to reservoir impact: dissolution of allochems and precipitation of calcite cements. Most dissolution is fabric-selective with allochems such as coral fragments, benthic foraminifera, and red algal grains commonly leached. Partial leaching of grains results in microporous textures, whereas complete leaching results in mold formation. Non-fabric-selective dissolution is commonly observed below interpreted exposure surfaces [4]. The dissolution/cementation below sequence boundaries is interpreted to be meteoric as it is associated with meteoric cement fabrics (cryptocrystalline meniscus, circumgranular, dog tooth, and blocky cements), and occurs prior to compaction. Fluid inclusion (brackish to fresh water inclusions) and stable isotopes (carbon and oxygen), following the meteoric or "inverted J" trend [5, 6], demonstrate that these cements have been formed by meteoric early diagenesis.

Most of the data points follow the burial trend

whereby variations in ^{13}C are minor compared to the overall variations in ^{18}O [34]. Later diagenetic dissolution of allochems rich in Mg-calcite (red algae and large benthic foraminifera) in the process of porosity inversion, might be driven by acidification of connate marine waters by CO_2 diffusion from the hydrocarbon reservoir down into the aquifer [35]. With the beginning of CO_2 and hydrocarbon charging the reservoir, the gas water contact and hence the dissolution of Mg-calcite-rich allochems moved downward, causing the amount of Ca^{2+}, CO_3^{2}, and also Mg^{2+} (mainly derived from dissolved corraline red algae) to increase in the underlying aquifer [36].

Partial dolomitisation, observed in the Serravallian section of both Well-2 and Well-3, is rare to non-existent in Well-4. Dolomitisation appears to post-date meteoric cement and pre-date deep burial-realm diagenesis. It is challenging to predict the extent of dolomitisation across the platform, given the limited number of well penetrations. Onset of clastic deposition occurred during the Tor1 sequence, constraining the initiation of dolomitisation to Early Tortonian time. Dolomitisation may continue to take place after initiation of burial by shales and marls, as tested in reactive transport modelling [37]. The observed partial dolomitisation at Well-2 and Well-3 might be related to CO_2 and hydrocarbon charging, causing secondary leaching of the Mg-rich coraline red algae and LBFs (see above). Enrichment of the water with Mg-ions might have favoured downward dolomitisation, driven by gas displacement, of the Serravallian carbonates [36]. This interpretation is supported by the fact that dolomitised sections of Well-2 and Well-3 are overlain by porous (leached) carbonates. It is important to note, that only Serravallian carbonates are dolomitised. Dolomitisation does not cross the Serravallian to Langhian boundary (Serravallian sequence boundary Ser1_SB). This argues for an internal and very local Mg source but might also be caused by the different grain composition of the Serravallian compared with the Langhian. The Langhian is dominated by aragonitic bioclasts like corals, whereas the Serravallian is dominated by bioclasts built by Mg-calcite, like coralline red algae. One might argue, that dolomitisation needs high-Mg calcite seeds or nucleation sites (missing in the Langhian) to trigger ("jump-start") dolomitisation [38, 39].

5. Reservoir rock types (RRT) and geologic controls on reservoir architecture

Reservoir rock typing was done in an effort to model varying reservoir quality, tied to different environments of deposition (EOD) across the Ca Voi Xanh platform. Reservoir rock types (RRT) were identified based on lithofacies, diagenesis, and reservoir parameters. Eight RRTs were identified: six in the Serravallian (RRT-1, RRT-2, RRT-3, RRT-4, RRT-5, and RRT-6; described in detail below) and two in the Langhian (RRT-3L and RRT-5L; Figure 5).

5.1. Reservoir rock type 1 (RRT-1)

RRT-1 (Figure 6) is limited to Well-2 core material (Figure 2). However, it also occurs as pre-dolomitised RRT-1 within the dolomitised part of Well-3 core material (Figure 2). This RRT is characterised by large benthic foraminifera (LBF), encrusting coralline red algae, and, often horizontally aligned, rhodoliths and platy corals. RRT-1 is the only

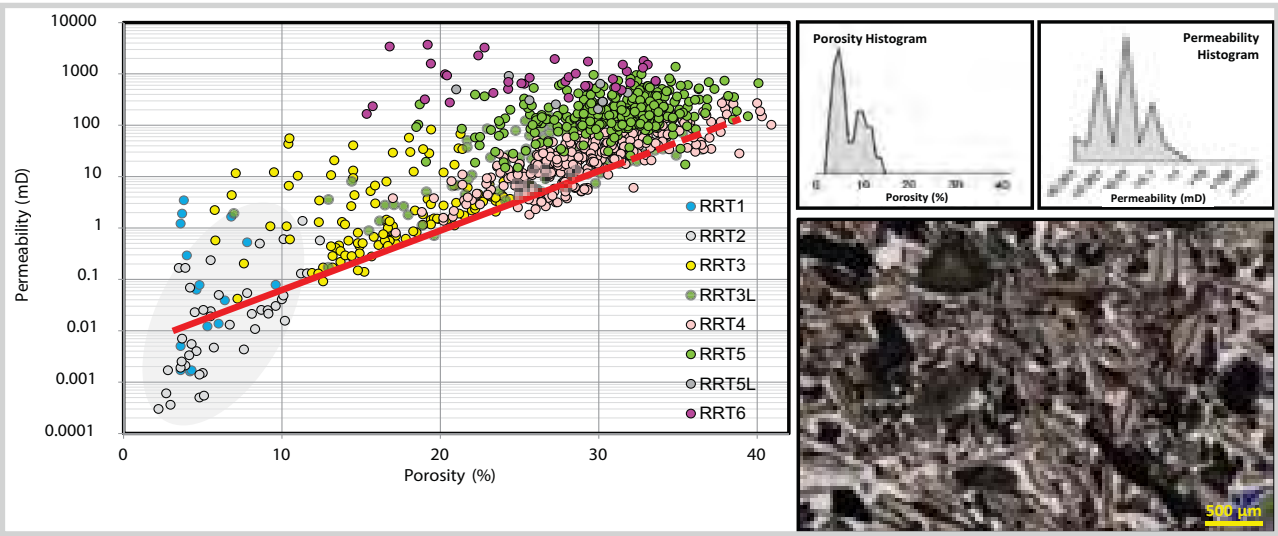

Figure 7. *Reservoir rock type 2. Displayed are permeability/porosity cross-plot (left) and porosity and permeability histograms, as well as thin section photomicrograph (right). Microporosity line (red), showing microporosity-dominated (below the red micro porosity line) and non-microporosity-dominated (above the red microporosity line) samples [40, 41].*

RRT that shows considerable amounts of mud, giving it a packstone to mud-lean packstone texture (LBF-rhodolith packstone to mud-lean-packstone). Compaction features like horizontal stylolites and solution seams are common.

RRT-1 is interpreted to represent a low-energy, deeper marine, distal middle shelf environment); most likely in an estimated 50 to 100m water depth range.

Throughout the Serravallian section at Well-2 and Well-3 (pre-dolomite RRT-1), intervals representing RRT-1 occur commonly around interpreted maximum flooding surfaces (MFS). This interpretation is further supported by biostratigraphy.

The pore system is dominated by microporosity [40, 41]. Subordinate partial moldic and between particle porosity is partly occluded by blocky calcite cement. RRT-1 is preferentially dolomitized (see RRT-4).

5.2. Reservoir rock type 2 (RRT-2)

RRT-2 (Figure 7) is present in core material of all three wells studied (Figure 2). It is made up of similar allochems characteristic for RRT-1 (but lacks considerable amounts of mud) and RRT-3. RRT-2 is described as rhodolith-LBF grainstone.

The graistone texture indicates elevated to high water-energy conditions. Environment of deposition (EOD) ranges from proximal to mid middle shelf, most probably representing rather shallow water depth of around 30m.

Cementation with circumgranular and blocky cement has considerably reduced between particle, partial moldic, and moldic pore space. Apparent microporosity (Figure 7) is within the grains. RRT-2 represents a strongly cemented version (strong diagenetic overprint) of RRT-3 (see below).

The presence of RRT-2 near interpreted sequence boundaries suggests that cementation most likely is related to exposure. This interpretation is further supported by the presence of cryptocristalline meniscus, circumgranular (but not isopachous), dog tooth, syntaxial, and blocky cements, as well as $\delta^{18}O$ and $\delta^{13}C$ isotope, and optical fluid inclusions (OFI) analyses; all indicating that cementation took place early in the meteoric phreatic diagenetic environment (Figure 4).

5.3. Reservoir rock type 3 (RRT-3)

RRT-3 (Figure 8) dominates the Seravallian section at Well-1, but it is also present, although to a lesser degree, at Well-3 and Well-4 (Figure 2). Similar to RRT-2, RRT-3 is described as rhodolith-LBF grainstone to mud-lean packstone.

Like RRT-2, RRT-3 is characterised by LBF (Cycloclypeus, Katacycloclypeus, Amphistegina, Lepidocyclina) and rhodoliths, interpreted to have been deposited throughout the proximal to distal middle shelf under moderate to high water-energy conditions. An absolute water depth is difficult to assign to this type of rhodolith-dominated carbonates. However, LBF assemblages, the occurrence of smaller benthic foraminifera, and rhodolith morphologies suggest that it may vary between 30 to 80m.

The pore system is dominated by between particle, partial moldic, and moldic porosity. Cement is present

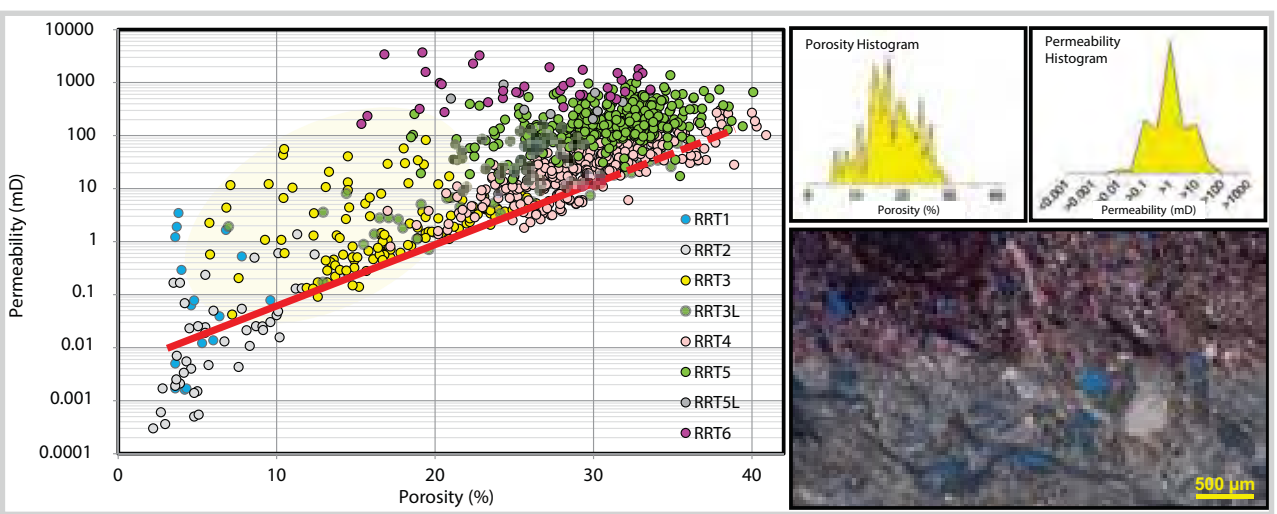

Figure 8. *Reservoir rock type 3. Displayed are permeability/porosity cross-plot (left) and porosity and permeability histograms, as well as thin section photomicrograph (right). Microporosity line (red), showing microporosity-dominated (below the red micro porosity line) and non-microporosity-dominated (above the red microporosity line) samples [40, 41].*

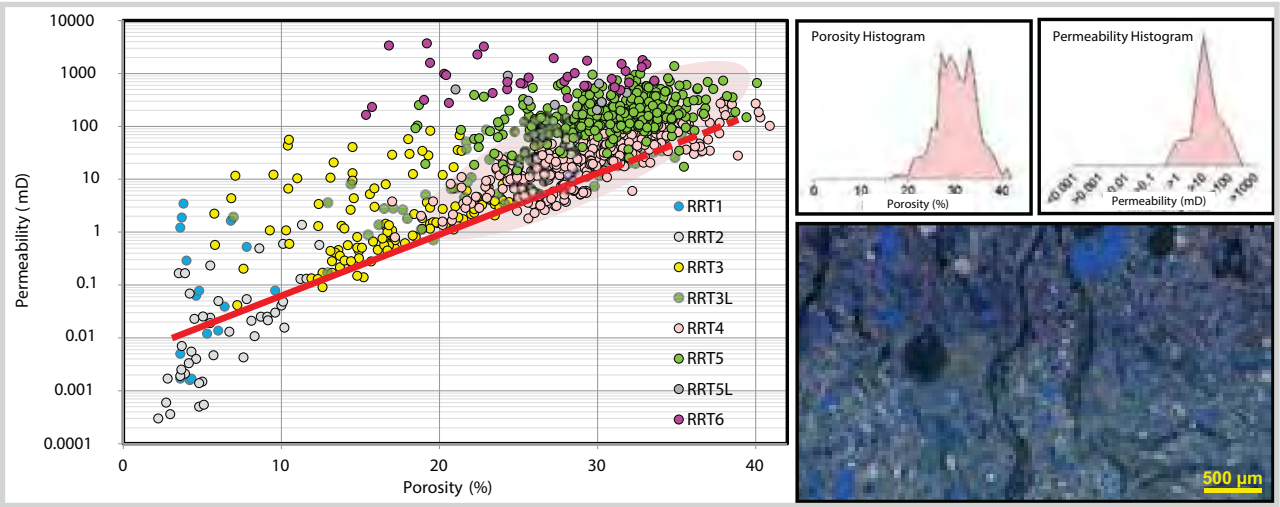

Figure 9. *Reservoir rock type 4. Displayed are permeability/porosity cross-plot (left) and porosity and permeability histograms, as well as thin section photomicrograph (right). Dolomite content is 87%. Microporosity line (red), showing microporosity-dominated (below the red micro porosity line) and non-microporosity-dominated (above the red microporosity line) samples [40, 41].*

(cryptocrystalline meniscus, circumgranular, isopachous, syntaxial, and blocky), but it does not occlude all pore space. Cement types represent marine vadose (cryptocrystalline meniscus cement), phreatic (isopachous, neomorphosed acicular aragonite, and bladed and high-Mg calcite cements), meteoric vadose (cryptocrystalline meniscus cement), phreatic (circumgranular, dog tooth and blocky, as well as syntaxial cements), and/or burial (syntaxial and blocky to drusy mosaic cements) diagenetic environments.

RRT-3 represents a depositional, minor diagenetically altered, reservoir rock type.

The presence or absence of the above-mentioned cement types is, however, responsible for the wide range in porosity and permeability.

5.4. Reservoir rock type 4 (RRT-4)

RRT-4 (Figure 9) is comprised of partially dolomitised carbonates and is limited to the Serravallian (not present at Well-4; Figure 2). RRT-4 is a diagenetic reservoir rock type, overprinting RRT-1, RRT-3, and RRT-5. RRT-4 is characterised as dolomitised samples with > 12% dolomite. Dolomitisation generally enhances reservoir quality with the exception of samples interpreted to represent dolomitised RRT-5. RRT-5 shows somewhat reduced porosities and permeabilities when dolomitised. However, overall reservoir quality remains very good.

The pore system is dominated by intercrystalline, between particle, partial moldic, and moldic porosity, as well as minor microporosity (Figure 7).

Sediment texture and structure-mimetic dolomitisation is interpreted to occur early in the burial history after early dissolution and phreatic cementation, but prior to stylolite formation and late cementation. This event was likely initiated between 10.5 and 10Ma during sea-level rise that followed platform exposure, causing platform-top flooding and eventual platform demise (drowning).

Numerous models exist, discribing various diagenetic environments where dolomitisation is interpreted to take place [42]. One interpretation is that the freshwater lens thickness, which is relatively easy to determine based on the exposed platform or island dimensions, acts as an insulator to the dolomitisation front. This scenario favours seawater being the most likely dolomitisation fluid. More recently, the hypothesis of dolomitisation from early CO_2 charge was proposed by Rivers et al. [36]. Post-burial rapid charge of hydrocarbon and CO_2 displaces connate water and causes dissolution of magnesium calcite at the gas-water contact; as described above. Dissolution of red algae (high-Mg calcite) and resulting Mg-ion concentration drives aqueous systems near the gas-water contact toward high-Mg calcite and dolomite saturation. Simulation and reactive transport modeling of CO_2 gas injection into carbonate reservoirs shows CO_2 can drive dissolution and density driven convective mixing [35]. Dolomitisation ceases abruptly at the Serravallian-Langhian boundary, supporting a local source of magnesium for dolomitisation and/or the interpretations that dolomitisation is triggered by high-Mg calcite (coralline red algae) or dolomite "seeds" (nucleation sites) in the sediment. Rivers et al. [36] concluded that dolomitisation appears to preferentially

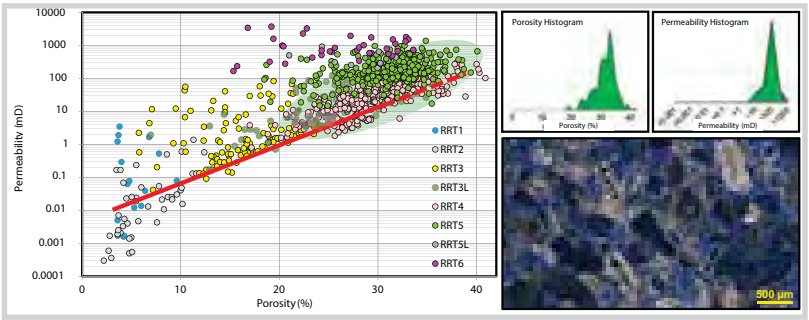

***Figure 10**. Reservoir rock type 5. Displayed are permeability/porosity cross-plot (left) and porosity and permeability histograms, as well as thin section photomicrograph (right). Microporosity line (red), showing microporosity-dominated (below the red micro porosity line) and non-microporosity-dominated (above the red microporosity line) samples [40, 41].*

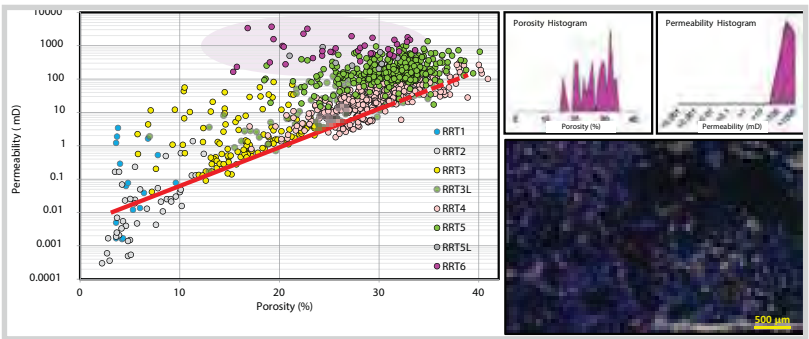

***Figure 11.** Reservoir rock type 6. Displayed are permeability/porosity cross-plot (left) and porosity and permability histograms, as well as thin section photomicrograph (right). Microporosity line (red), showing microporosity-dominated (below the red micro porosity line) and non-microporosity-dominated (above the red microporosity line) samples [40, 41].*

affect mud-dominated facies. To test this interpretation, pre-dolomite RRTs were interpreted from core and thin sections of Well-2 and Well-3. The results support the initial conclusions made by Rivers et al. [36].

5.5. Reservoir rock type 5 (RRT-5)

Like RRT-3, RRT-5 (Figure 10) is dominantly a rhodolith-LBF grainstone. It dominates Well-3 and Well-4, and, to a minor degree, Well-2 (Figure 2).

RRT-5 can be described as a diagenetically altered (leached) RRT-3. The pore system includes between particle, partial moldic, moldic, as well as minor non-fabric selective vuggy porosity; the latter showing touching vugs. Dominant cement type is meteoric circumgranualar cement. Syntaxial and blocky cements (meteoric and/or shallow burial cements) are less common.

RRT-5 is interpreted to be the result of early meteoric dissolution, most probably related to exposure, and subsequent minor cementation in the meteoric phreatic zone. Later diagenetic, CO_2-related dissolution, might have additionally increased porosity.

5.6. Reservoir rock type 6 (RRT-6)

Like reservoir rock types RRT-3 and RRT-5, RRT-6 (Figure 11) is described as a rhodolith-LBF grainstone, representing a diagenetically altered (leached) RRT-3. Its vertical distribution is limited to the top of the Serravallian at Well-3 and Well-4 (Figure 2). RRT-6 samples show no cementation, but enhanced leaching.

The pore system is dominated by vuggy (touching vugs), partial moldic, moldic, and between partical porosity. The occurrence of touching vugs and the lack of cementation considerably enhances the permeability of RRT-6, compared to all other reservoir rock types.

Like RRT-5, RRT-6 is interpreted to represent early diagenetic, meteoric leaching of the carbonates, related to exposure (epikarst). However, later diagenetic leaching during burial, related to CO_2 invasion is also possible.

6. 3D Seismic Paleo-Structure and Karst Mapping

Paleo-structure reconstructions, showing the antecedent topography of the Ca Voi Xanh platform, can be used to spatially guide the distribution of RRTs. Topographic lows (deeper water) would have a higher probability of being occupied by RRT-1, whereas topographic highs (shallower water) would have a higher probability of being occupied by RRT-3.

Paleo-structure, in conjunction with seismically observed karst can also be used to define potential areas of exposure at top carbonate (Tor1_SB). The extent of exposure is a key control on distribution and probability of meteoric diagenesis associated with RRT-5 and RRT-6.

Two seismic horizons were selected that, when used as a datum, best represent the paleo-structure (antecedent topography) at the onset of Serravallian carbonate depostion and at the time of subsequent exposure at top carbonate (Tor1_SB).

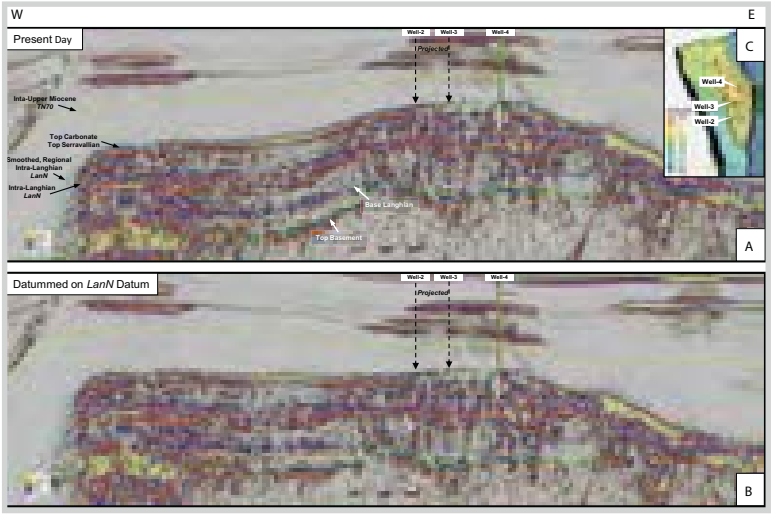

Figure 12. *Seismic section showing present day structure (a). Seismic section showing paleo-structure reconstruction using intra-Langhian seismic horizon LanN as datum (b). Paleo-structure map showing position of seismic section shown on Figures 12a and 12b (c).*

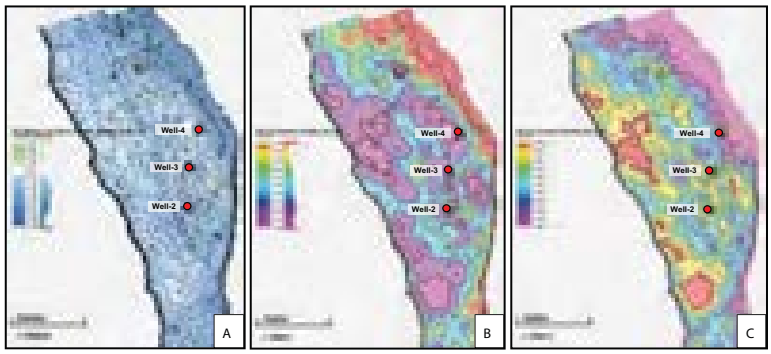

Figure 13. *Serravallian paleo-structure map datummed on Langhian seismic horizon LanN (a). RRT-1 probability map (geologic model zone 2) showing high RRT-1 probability corresponding to topographic lows (darker blue areas: deeper water) (b). RRT-3 probability map (geologic model zone 2) showing high RRT-3 probability corresponding to topographic highs (lighter blue/whitish areas: shallower water) (c).*

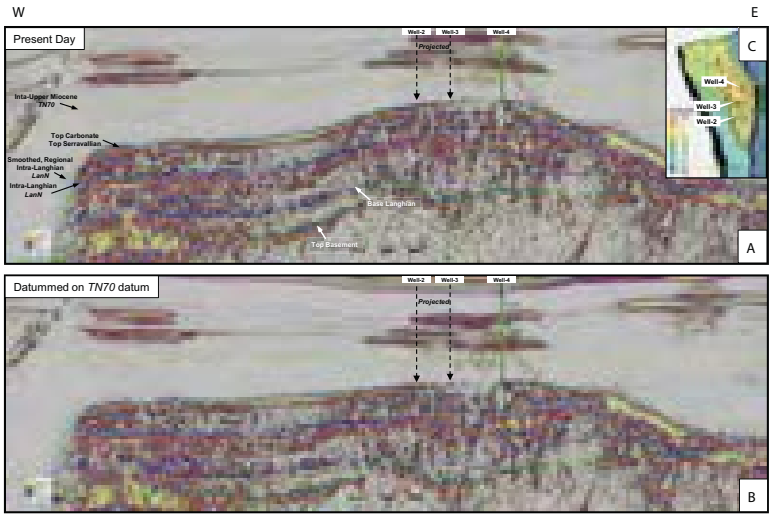

Figure 14. *Seismic section showing present day structure (a). Seismic section showing paleo-structure reconstruction using intra-Upper Miocene horizon TN70 as datum. (b) Paleo-structure map showing position of seismic sections shown on Figures 14a and 14b (c).*

An intra-Langhian seismic horizon (LanN) was used as datum for representing the paleo-structure (paleo-topography) at the onset of Serravalllian carbonate deposition (Figure 12). It is an interpretive smooth surface, based on anchoring sea-level in areas of strong constructional/aggradational facies on the western and eastern carbonate margins, and interpreting/interpolating paleo-water depth in between these anchor points. The selected surface is one of multiple possible realisations.

Figure 13 shows probability maps of RRT-1 and RRT-3 distribution throughout the lower part of the Serravallian; related to the constructed paleo-structure map. Topographic lows or somewhat deeper water conditions (Figure 13a) correspond to a high probablilty of RRT-1 occurrence (Figure 13b), whereas topographic highs or somewhat shallower water conditions (Figure 13a) correspond to a high probablility of RRT-3 occurrence (Figure 13c).

Within the overburden, an intra-Upper Miocene horizon (TN70) was used to show the inferred extent of exposure at top carbonate (Tortonian paleo-structure; Figure 14). It is a relatively well-defined seismic surface at the top of homogeneous marine shales encountered in all Ca Voi Xanh wells. Below this horizon, the clastic section shows significant thickening due to progradation and loading from the west and southwest.

Figure 15 shows a probability map of RRT-5 and RRT-6 distribution throughout the upper part of the Serravallian; related to the re-constructed Tortonian paleo-structure map. Structural highs (Figure 15a) correspond to more exposure and higher probability of RRT-5 and RRT-6 (Figure 15b). On the contrary, structural lows correspond to less exposure and lower probability of RRT-5 and RRT-6 (Figure 15b).

Observations from the 3D seismic data indicate that there is an extensive

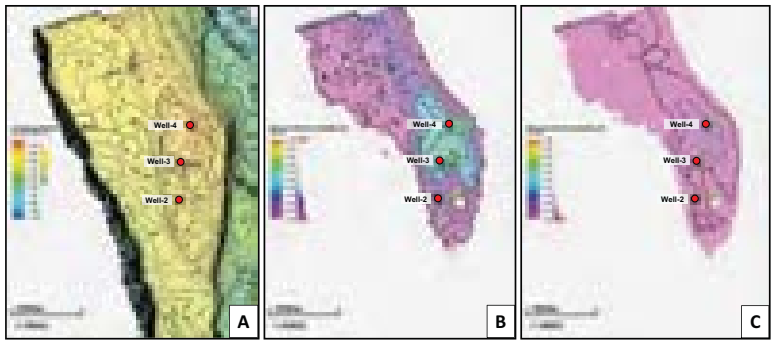

Figure 15. *Tortonian paleo-structure map datummed on Upper Miocene seismic horizon TN70 (a). RRT-5 probability map (geologic model zone 3) showing high RRT-5 probability corresponding to structural high areas (b). RRT-6 probability map (geologic model zone 3) showing high RRT-6 probability corresponding to structural high areas (c).*

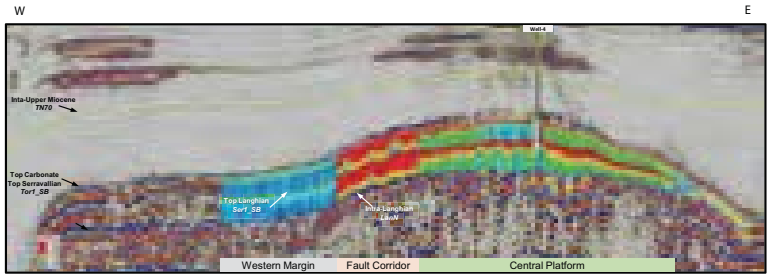

Figure 17. *Seismic-conditioned karst density probability (hot colours corresponding to high density probability) co-rendered over seismic section (position shown on Figure 16); following sequence boundaries Ser1_SB and Tor1_SB. Highest karst density probability is directly below sequence boundaries Ser1_SB and Tor1_SB along the Central Platform. Fault Corridor shows highest vertical karst/fracture density. Less karst/fracture density characterises the area of the Western Margin.*

karst network on the Ca Voi Xanh structure (Figure 16). Different karst geometries and features consistent with known hydro-geologic processes are identified in the seismic discontinuity cube (variance cube) and are used to interpret karst regions (Figure 17). A variance volume draped on the top carbonate structure map illustrates discontinuities in the seismic data, interpreted to be karst-related features (Figure 16). Observations from seismic data indicate that the platform was not karsted uniformly. There is a high-density network of karst features in the northern part of the platform, but they are more sparsely distributed in the central and western areas. Reduced imaging quality underneath gas-filled siltstones makes it difficult to determine the extent of the karst network around Well-2 and Well-3 in the main field area (Figure 16). Vertical trends in karst density honour the Ser1_SB and Tor1_SB sequence boundaries, resulting in more karst/fractures being populated near these interpreted exposure surfaces (Figure 17). Karst characterisation comprises the non-matrix component of the geologic model [43, 44].

7. Conclusions

Offshore Da Nang (Central Vietnam), Middle Miocene (Langhian and Serravallian) carbonates build the reservoir of the isolated Ca Voi Xanh platform; nucleating on top of the north-south striking Tri Ton horst (Figure 1).

Serravallian carbonates can be described by one third-order

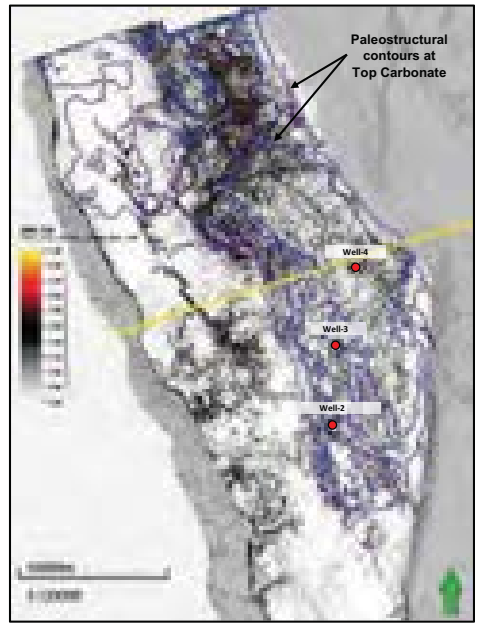

Figure 16. *Variance volume draped on top carbonate structure map shows reasonable agreement between paleo-structural top carbonate highs and extent of dense seismically observed karst. Overall density of karst appears to lessen southwards, consistent with the interpretation of being paleo-structurally deeper, but complicated by data quality degradation beneath overlaying gas-filled siltstones. Pattern of western platform/margin karst typical of tidal channels (in paleo-structural lows) consistent with minimal/no exposure of western margin due to structural subsidence at that time. Blue contour line indicates area with greatest intensity of karst network (longest residence time in the meteoric realm). Yellow line shows position of seismic section shown on Figure 17.*

composite sequence, comprising three third-order depositional sequences. Four major, regionally correlative sequence stratigraphic surfaces, can be carried across the Ca Voi Xanh platform (Figure 2).

Langhian carbonates are characterized by a photozoan grain association, dominated by hermatipic corals, large benthic (Miogypsina) and, predominantly, small benthic foraminifera, including miliolids, soritids, and alveolinids. A warm, shallow marine, inner shelf environment of deposition is inferred for the Langhian carbonates.

Serravallian carbonates are interpreted to represent a deeper open marine, proximal to distal middle ramp environment. The carbonates are rich in large benthic foraminifera (LBF). Serravallian carbonates represent a typical heterozoan association

of organisms.

Early and later diagenetic events rather than primary depositional facies mainly influence reservoir properties. Early, meteoric diagenesis (both vadose and phreatic) is tied to exposure of the carbonates, due to pronounced sea-level falls at the end of Langhian and Serravallian times (Figures 3 and 4). Cement types (cryptocrystalline meniscus, circumgranular, dog tooth, and blocky cements), fluid inclusion and stable isotopes, following the "inverted J" trend, support the interpretation that the carbonates were overprinted by meteoric diagenesis below sequence boundaries (Figure 4b and 4c).

Later diagenetic dissolution of Serravallian allochems rich in Mg-calcite (coralline red algae, and large benthic foraminifera) in the process of porosity inversion, might be driven by acidification of connate marine waters by CO_2 diffusion from the hydrocarbon reservoir down into the aquifer.

Partial dolomitisation of Serravallian carbonates, observed at Well-2 and Well-3, is interpreted to be related to CO_2 and hydrocarbon charging, causing secondary leaching of the Mg-rich coralline red algae and LBFs. This leads to the enrichment of the water with Mg-ions, favoring downward dolomitisation of Serravallian carbonates. The fact that dolomitisation does not cross the Serravallian to Langhian sequence boundary Ser1_SB argues for an internal and very local Mg source, but can also be controlled by the different grain composition of the Serravallian (high-Mg calcite dominated mineralogy) compared with the Langhian (aragonite dominated mineralogy). Dolomitisation of Serravallian carbonates is thought to be triggered by high-Mg calcite seeds or nucleation sites, missing in the Langhian.

A reproducible reservoir rock type (RRT) scheme was developed for Langhian and Serravallian carbonates, using a combination of depositional environment, diagenetic overprint, and reservoir parameters (Figure 5). The Langhian is characterised by two RRTs, depending on the degree of cementation (RRT-3L) and dissolution (RRT-5L). The Serravallian RRTs are separated into dominantly packstone (RRT-1; Figure 6) and dominantly grainstone textures (RRT-2, RRT-3, RRT-5, and RRT-6; Figures 7, 8, 10, and 11). RRTs with grainstone texture show varying degrees of cementation (RRT-2 and RRT-3; Figures 7 and 8) and dissolution (RRT-5 and RRT-6, Figures 10 and 11). Reservoir rock type RRT-4 is a diagenetic RRT, showing partial dolomitisation (>12%; Figure 9). The vertical and lateral distribution of RRTs, supported by seismically-derived paleo-reconstruction of the carbonate platform, adequately describes the matrix component of the Ca Voi Xanh reservoir.

Different karst geometries and features identified in the seismic discontinuity (variance) cube (Figure 16) are used to interpret karst regions with different degrees and/or types of karst. These karst regions are used to populate the non-matrix component of the geologic model. Vertical trendology of karst distribution follows sequence boundaries Ser1_SB and Tor1_SB, populating more karst/fractures near these interpreted exposure surfaces (Figure 17).

Acknowledgements

The authors gratefully acknowledge the management of the Vietnam Oil and Gas Group (PVN), Petrovietnam Exploration Production Corporation, ExxonMobil Exploration & Production Vietnam Ltd., and Esso Australia Pty. Ltd. for permission to publish this paper.

We thank Han van Gorsal for identifying the large benthic foraminifera (LBF) and Davide Bassi for his input on the paleoenvironmental settings of fossil coralline red algal assemblages.

References

1. Michael B.W.Fyhn, Lars O.Boldreela, Lars H.Nielsen, Tran C.Giang, Le H.Nga, Nguyen T.M.Hong, Nguyen D.Nguyen, Ioannis Abatzis. *Carbonate platform growth and demise offshore Central Vietnam: Effects of Early Miocene transgression and subsequent onshore uplift*. Journal of Asian Earth Sciences. 2013; 76: p. 152 - 168.

2. Trinh Xuan Cuong, Vu The Anh, Le Chi Mai. *Tectonic development of the Tri Ton horst and Adjacent areas, offshore South Vietnam*. AAPG Datapages/Search and Discovery Article #90236, Asia Pacific Region, Geoscience Technology Workshop, Tectonic Evolution and Sedimentation of South China Sea Region, Kota Kinabalu, Sabah, Malaysia. 26 - 27 May, 2015.

3. J.F.Sarg, J.R.Markello, L.J.Weber. *The second-order cycle, carbonate-platform growth, and reservoir, source, and trap prediction*. Advances in carbonate sequence stratigraphy: Application to reservoirs, outcrops and models. SEPM Special Publication. 1999; 63: p. 11 - 34.

4. Mateu Esteban, Colin F.Klappa. *Subaerial exposure environment. Carbonate depositional environments*. American Association of Petroleum Geologists. 1983.

5. K.C.Lohmann. *Inverted "J" carbon and oxygen isotopic trends: A criterion for shallow meteoric phreatic diagenesis*. Geological Society of America, Abstracts and Program. 1982; 14: p. 548.

6. Kyger C.Lohmann. *Geochemical patterns of meteoric diagenetic systems and their application to studies of paleokarst*. Paleokarst. Springer. 1988: p. 58 - 80.

7. A.R.Isern, F.S.Anselmetti, P.Blum. *Constraining Miocene sea level change from carbonate platform evolution, Marion Plateau, Northeast Australia*. Initial Reports, Ocean Drilling Program. 28 March 2002; 194.

8. Brian Jones. *Warm-water neritic carbonates*. Facies Models 4. Geological Association of Canada. 2010: p. 341 - 370.

9. Noel P.James, R.A.Wood. *Reefs.* Facies Models 4. Geological Association of Canada, 2010: p. 421 - 448.

10. N.P.James. *The cool-water depositional realm.* Cool-water carbonates. Society of Economic Paleontologists and Mineralogists Special Publication. 1997; 56: p. 1 - 20.

11. D.Bassi. *Paleoenvironmental settings of fossil coralline red algal Assemblages*. ExxonMobil Internal Report. 2016.

12. W.H.Adey, I.G.McIntyre. *Crustose coralline algae: a re-evaluation in the geological sciences*. Bulletin Geological Society of America, 1973; 84: p. 883 - 903.

13. W.H.Adey. *Crustose coralline algae as microenvironmentai indicators in the Tertiary. Historical biogeography, plate tectonics and the changing environment*. Oregon State University Press. 1979: p. 459 - 464.

14. J.M.Martin, J.C.Braga. *Eocene to Pliocene coralline algae in the Queensland Plateau (Northeastern Australia*). Proceedings of the Ocean Drilling Program, Scientific Results, College Station. 1993; 133: p. 67 - 74.

15. J.M.Martin, J.C.Braga, K.Konishi, C.J.Pigram. *A model for the development of rhodoliths on platforms influenced by storms: Middle Miocene carbonates of the Marion Plateau (Northeastern Australia)*. Proceedings of the Ocean Drilling Program, Scientific Results, College Station. 1993; 133: p. 455 - 460.

16. W.H.Adey, R.A.Townsend, W.T.Boykins. *The crustose coralline algae (Rhodophyta: Corallinaceae) of the Hawaiian islands*. Smithsonian Contributions to the Marine Sciences. 1982; 15: p. 1 - 74.

17. Y.Tsuji. *Tide influenced high energy environments and rhodolith-associated carbonate deposition on the outer shelf and slope of Miyako islands, southern Ryukyu island Arc*. Marine Geology. 1993; 113: p. 255 - 271.

18. S.Matsuda, Y.Iryu. *Rhodoliths from deep fore-reef to shelf areas around Okinawa-jima, Ryukyu islands, Japan*. Marine Geology. 2011; 282: p. 215 - 230.

19. Y.Iryu, T.Nakamori, S.Matsuda, O.Abe. *Distribution of marine organisms and its geological significance in the modern reef complex of the Ryukyu Islands*. Sedimentary Geology. 1995; 99: p. 243 - 258.

20. J.M.Webster, L.Fallace, E.Silver, D.Potts, J.C.Braga, W.Renema, K.Riker-Coleman, C.Gallup. *Coralgal composition of drowned carbonate platforms in the Huon Gulf, Papua New Guinea; implications for lowstand reef development and drowning*. Marine Geology. 2004; 204: p. 59 - 89.

21. G.A.Minnery. *Crustose coralline algae from the Flower Garden Banks, northwestern Gulf of Mexico: Controls on distribution and growth morphology*. Journal of Sedimentary Petrology. 1990; 60: p. 992 - 1007.

22. C.Perrin, D.Bosence, B.Rosen. *Quantitative approaches to paleozonation and paleobathymetry of corals and coralline algae in Cenozoic reefs.* Marine paleoenvironmental analysis from fossils. Geological Society, London, Special Publications. 1995; 83: p. 181 - 229.

23. F.T.S.Tâmega, M.A.O.Figueiredo. *Distribuiçäo das algas calcárias incrustantes (Corallinales, Rhodophyta) em diferentes habitats na Praoa Do Forno, Amaçäo dos Búzios, Rio de Janeiro*. Rodriguésia. 2005; 56: p. 123 - 132.

24. D.S.Littler, M.M.Littler. *South Pacific reef plants. A divers' guide to the plant life of South Pacific coral reefs*. Offshore Graphics, Inc., Washington. 2003; 332p.

25. W.J.Woelkerling. *Subfamily Mastophoroideae Setchell 1943. The marine benthic flora of Southern Australia. Part IIIB: Gracilariales, Rhodymeniales, Corallinales and Bonnemaisoniales*. Australian Biological Resources Study, Canberra. 1996: p. 237 - 283.

26. A.S.Harvey, W.J.Woelkerling, T.Farr, K.Neill, W.Nelson. *Coralline algae of central New Zealand. An identification guide to common 'crustose' species*. National Institute of Water and Atmospheric Research Information Series, Wellington, New Zealand. 2005; 57: 145p.

27. J.C.Braga, D.Bassi. *Neogene history of Sporolithon*

Heydrich (Corallinales, Rhodophyta) in the Mediterranean region. Palaeogeography, Palaeoclimatology, Palaeoecology. 2007; 243: p. 189 - 203.

28. G.A.Minnery, R.Rezak, T.J.Bright. *Depth zonation and growth form of crustose coralline algae: Flower Garden Banks, northwestern Gulf of Mexico*. Paleoalgology. Springer-Verlag, Berlin. 1985: p. 237 - 247.

29. R.A.Townsend, W.J.Woelkerling, A.S.Harvey, M.Borowitza. *An account of the red algal genus Sporolithon (Sporolithaceae, Corallinales) in southern Australia*. Australian Systematic Botany. 1995; 8: p. 85 - 121.

30. D.Basso, R.Nalin, C.S.Nelson. *Shallow-water Sporolithon rhodoliths from North island (New Zealand). Palaios*. 2009; 24: p. 92 - 103.

31. P.Kindler, C.Ruchonnet, T.White. *The Southern Marion Platform (Marion Plateau, NE Australia) during the early Pliocene: A lowstand-producing, temperate-water carbonate factory*. Cool-water carbonates: Depositional systems and palaeoenvironmental controls. Geological Society, London, Special Publications. 2006; 255: p. 269 - 282.

32. D.Bassi, Y.Iryu, M.Humblet, H.Matsuda, H.Machiyama, K.Sasakl, S.Matsuda, K.Arai, T.Inoue. *Recent macroids on the Kikai-jima shelf, Central Ryukyu islands, Japan*. Sedimentology. 2012; 59: p. 2024 - 2041.

33. A.Mewes, G.Langer, S.Thoms, G.Nehrke, J.Reichart, L.J.De Nooijer, J.Bijma. *Impact of seawater [Ca^{2+}] on the calcification and calcite Mg/Ca of Amphistegina lessonii*. Biogeosciences. 2015; 12: p. 2153 - 2162.

34. P.W.Choquette, N.P.James. *Limestones - The burial diagenetic environment*. Diagenesis. Geoscience Canada, Reprint Series 4. 1990: p. 75 - 112.

35. Y.Xiao, G.Macleod, D.M.Advocate, C.Reaves, R. J.Pottorf. *Natural CO_2 occurrence in geological formations and the implications on CO_2 storage capacity and site selection*. Energy Procedia. 2011; 4: p. 4688 - 4695.

36. J.Mrivers, L.Meyer, D.Walley, J.Anthony, S.Becker. *Depositional and diagenetic investigation of a Tertiary isolated carbonate platform, evidence for significant gas-charge-related dolomitization*. AAPG Datapages/Search and Discovery Article #90259, AAPG Annual Convention and Exhibition, Calgary. 2016.

37. F.F.Whitaker, Y.Xiao. *Reactive transport modeling of early burial dolomitization of carbonate platforms by geothermal convection*. AAPG Bulletin. 2010; 94: p. 889 - 917.

38. C.J.Strohmenger, F.Sadooni, T.R.R.Bontognali, J.A.Mckenzie, C.Vasconcelos. *Microbial-mediated dolomite from coastal sabkha environments of Abu Dhabi and Qatar: Analogues to subsurface arid climate dolomitized reservoir rocks*. AAPG Search and Discovery Article #90189, AAPG 2014 Annual Convention and Exhibition, Houston. 2014.

39. F.Sadooni, C.J.Strohmenger, T.R.R.Bontognali, J.A.Mckenzie, C.Vasconcelos. *Possible microbial origin of ancient dolomites formed under arid climatic conditions: A geo-microbiological approach*. 15th Bathurst Meeting, Edinburgh. 2015: p. 96 - 97.

40. S.M.Fullmer, S.A.Guidry, J.Gournay, E.Bowlin, G.Ottinger, A.Al Neyadi. *Microporosity: Characterization, distribution, and influence on oil recovery*. Abu Dhabi International Petroleum Conference and Exhibition, Abu Dhabi, UAE. 2014.

41. S.E.Kaczmarek, S.M.Fullmer, F.J.Hasiuk. *A universal classification scheme for the microcrystals that host limestone microporosity*. Journal of Sedimentary Research. 2015; 85: p. 1197 - 1212.

42. H.G.Machel. *Concepts and models of dolomitization: A critical reappraisal. The geometry and petrogenesis of dolomite hydrocarbon reservoirs*. Geological Society, London, Special Publications. 2004; 235: p. 7 - 63.

43. A.Medekenova, G.D.Jones. *Characterization and modeling challenges associated with fracture and karst (non-matrix) in the margin area of a carbonate reservoir*. SPE Annual Caspian Technology Conference and Exhibition, Astana, Kazakhstan. 2014.

44. D.Abishev, A.Kassenov. *The evaluation of karst in the non-matrix model of carbonate reservoir*. SPE Annual Caspian Technology Conference and Exhibition, Astana, Kazakhstan. 2016.